Inorganic Chemistry

pubs.acs.org/IC

Article

Glucosyl Platinum(II) Complexes Inhibit Aggregation of the C-Terminal Region of the Aβ Peptide

Sara La Manna, Marilisa Leone, Ilaria Iacobucci, Alfonso Annuziata, Concetta Di Natale, Elena Lagreca, Anna Maria Malfitano, Francesco Ruffo, Antonello Merlino, Maria Monti,* and Daniela Marasco*

Cite This: *Inorg. Chem.* 2022, 61, 3540−3552

Read Online

ACCESS | Metrics & More | Article Recommendations | Supporting Information

ABSTRACT: Neurodegenerative diseases are often caused by uncontrolled amyloid aggregation. Hence, many drug discovery processes are oriented to evaluate new compounds that are able to modulate self-recognition mechanisms. Herein, two related glycoconjugate pentacoordinate Pt(II) complexes were analyzed in their capacity to affect the self-aggregation processes of two amyloidogenic fragments, $A\beta_{21-40}$ and $A\beta_{25-35}$, of the C-terminal region of the β-amyloid (Aβ) peptide, the major component of Alzheimer's disease (AD) neuronal plaques. The most water-soluble complex, $\mathbf{1Pt_{dep}}$, is able to bind both fragments and to deeply influence the morphology of peptide aggregates. Thioflavin T (ThT) binding assays, electrospray ionization mass spectrometry (ESI-MS), and ultraviolet−visible (UV−vis) absorption spectroscopy indicated that $\mathbf{1Pt_{dep}}$ shows different kinetics and mechanisms of inhibition toward the two sequences and demonstrated that the peptide aggregation inhibition is associated with a direct coordinative bond of the compound metal center to the peptides. These data support the *in vitro* ability of pentacoordinate Pt(II) complexes to inhibit the formation of amyloid aggregates and pave the way for the application of this class of compounds as potential neurotherapeutics.

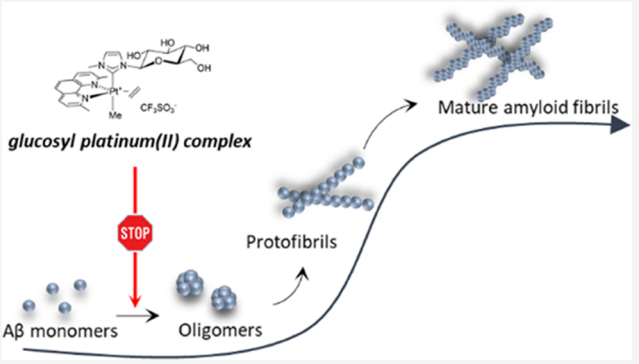

INTRODUCTION

In Alzheimer's disease (AD) pathophysiology, the β-amyloid (Aβ) peptide represents the prevalent component of senile plaques[1] even if it is present at the early phases of life, and in its monomeric form, it can act as a positive regulator of the presynaptic release in hippocampal neurons.[2] Aβ is a polypeptide spanning 1−40 or 42 residues that is mostly intrinsically disordered.[3] Through a self-assembly process that is typical of amyloid aggregation, it forms different Aβ oligomers, endowed with diverse levels of order that represent key pathogenic species in AD.[4] Amyloid assemblies induce synaptic dysfunction and neuronal death[5] and oxidative damage and inflammation, which further corroborate the progression of the disease.[6] The presence of metals like Zn, Fe, Cu, and Al inside amyloid plaques enhances Aβ-induced oxidative damage and its aggregation level; thus, a chelation approach to directly target metals in the brain can be conceived as a way to reduce harmful consequences of metal/fibril accumulation.[7] However, the most powerful therapeutic approach for AD is based on the inhibition of the aggregation of the Aβ peptide[8] and great efforts have been devoted to the identification of molecules capable of inhibiting its self-recognition. It has been shown that these compounds can have different origins (synthetic, natural) and chemical nature (phenols, peptide, antibodies, small molecules, *etc.*).[9−12] Even though many trials are actually ongoing, especially on natural compounds,[13] no drugs have entered into clinical use yet: this can be mainly due to the inability of targeting protein interfaces without regular secondary structures that could be assumed as templates to design inhibitors.[14,15] Recently, multivalent systems (as dendrimers) were investigated to gain access to different protein subregions.[16] Indeed, different Aβ regions contribute to amyloid aggregation: the N-terminus,[17] hydrophobic core,[18] so-called hinge and turn regions,[19] and C-terminus.[20,21] Experimental data indicated that the C-terminal region of Aβ can be addressed by the cyclohexanehexol scaffold: indeed, the scyllo-inositol compound interferes with the fibrillization process and competes with endogenous phosphatidylinositol for binding to the Aβ polypeptide, appearing as a promising therapeutic agent, currently in Phase II trials.[22]

The unique properties exhibited by transition-metal complexes as drugs, including their tunability in the oxidation

Received: November 12, 2021
Published: February 16, 2022

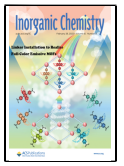

https://doi.org/10.1021/acs.inorgchem.1c03540
Inorg. Chem. 2022, 61, 3540−3552

Table 1. Sequences of the $A\beta_{1-42}$ Peptide and Peptides Investigated in this Study and Derived from its C-Terminal Domain

Peptide	Sequence
$A\beta_{1-42}$	DAEFRHDSGYEVHHQKLVFFAEDVGSNKGAIIGLMVGGVVIA
$A\beta_{21-40}$	AEDVGSNKGAIIGLMVGGVV
$A\beta_{25-35}$	GSNKGAIIGLM

and the coordination states, allow them to enter into many pharmaceutical applications.[23−25] In the amyloid context, they can be considered as good starting compounds for the development of novel neuroprotective agents.[26,27] The stability and inertness of Pt(II) and Ru(III)[28] complexes allowed a wide range of investigations with different amyloid systems: phenanthroline (phen)−Pt(II) complexes with two monodentate ligands (*e.g.*, chlorides) inhibit the aggregation of $A\beta_{1-40}$ and its N-terminal region[29−31] as well as of prion protein (PrP) fragments.[32,33] Polyoxometalate derivatives of Pt[34] and V[35] suppress amyloid aggregation in a mechanism involving multiple interactions: (i) the coordination of the metal, (ii) electrostatic, (iii) hydrogen, and (iv) van der Waals forces. Octahedral Co compounds,[36] as well as square-planar Pt complexes bearing polyaromatic ligands, interact with the Aβ peptide *via* $\pi-\pi$ stacking.[37] Furthermore, hetero-multinuclear Pt−Ru complexes are able to revert amyloidosis: they regulate amyloid-induced cytotoxicity in insulinoma β-cells and significantly increase cell viability.[38] Traditionally, due to the presence of His residues in its sequence, the N-terminal region of the Aβ peptide was considered the main target for inhibition studies of Aβ aggregation by metal compounds.[39] Conversely, with the aim to deepen the druggability of C-terminus by transition-metal complexes, in our recent investigations we assumed as amyloid model the fragment spanning residues 21−40 of Aβ ($A\beta_{21-40}$, Table 1),[40−42] which is also deeply involved in the mechanism of aggregation of the entire Aβ peptide. Herein, we also studied the behavior of a shorter Aβ fragment spanning residues 25−35 ($A\beta_{25-35}$, Table 1). It has been shown that this peptide is the most cytotoxic among the known Aβ peptides.[43]

Very recently, we have investigated the ability of a series of square-planar Pt(II) complexes to inhibit the aggregation of amyloid peptides.[40−42] Among the investigated systems, the pyridine-based platinum(II) complex, called Pt-terpy, exhibited good inhibitory effects of amyloid aggregation, also allowing, for its better water solubility when compared to other investigated complexes, to get insights into the mechanism of action of these types of molecules: the presence of the Pt complex stabilized soluble β-structures of the $A\beta_{21-40}$ peptide.[44] Some of us also designed new pentacoordinate glycoconjugate platinum(II) complexes that can act as anticancer compounds.[45] Sugar ligands were introduced aiming to enhance their biocompatibility, aqueous solubility, and recognition by cancer cells through the "Warburg effect".[46,47] The coordinative saturation is also an important stereoelectronic requisite that improves their general stability. In particular, the peracetylated NHC complex **1Pt** in Figure 1, prepared along with its deprotected counterpart $\mathbf{1Pt_{dep}}$, showed high activity and selectivity toward a panel of cell lines.[48]

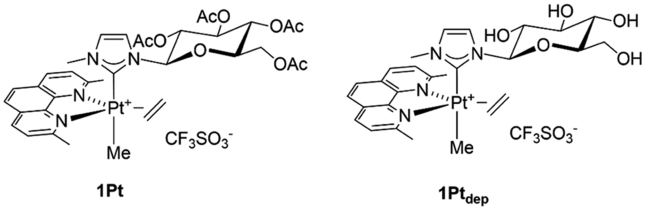

Figure 1. Pentacoordinate platinum(II) complexes **1Pt** and $\mathbf{1Pt_{dep}}$.

Here, we present investigations focused on the ability of the two complexes to act as effective inhibitors of aggregation of Aβ peptides reported in Table 1. The ability of $\mathbf{1Pt_{dep}}$ to inhibit the aggregation of Aβ peptides was confirmed *via* a range of spectroscopic and biophysical techniques.

RESULTS AND DISCUSSION

Effects of Pt Complexes on the Thioflavin T (ThT) Assay of $A\beta_{21-40}$ and $A\beta_{25-35}$. Spectroscopic investigations provided evidence of the ability of both **1Pt** and $\mathbf{1Pt_{dep}}$ to modulate the amyloid aggregation of Aβ-derived peptides. Initially, ThT was employed as a typical amyloid dye, which is able to bind to amyloid prefibrils, inducing a strong fluorescence signal at ∼482 nm when excited at 440 nm.[49,50] The overlays of ThT fluorescence emission profiles of the investigated peptides in the absence and presence of **1Pt** and $\mathbf{1Pt_{dep}}$ over time are reported in Figure 2.

Aβ peptide aggregation was investigated in the presence of metal complexes at peptide-to-metal molar ratios of 1:1 and 1:5. A reduction of aggregation in the presence of metal compounds is observed for almost all samples; fluorescence quenching is more evident in the case of $A\beta_{25-35}$. Comparing the effects of Pt complexes on the $A\beta_{21-40}$ aggregation, $\mathbf{1Pt_{dep}}$ exhibits greater suppressive effects (Figure 2A) with respect to **1Pt** (Figure 2C). $\mathbf{1Pt_{dep}}$ decreases aggregation of 60 and 90% at 1:1 and 1:5 peptide-to-metal molar ratios, respectively. Under similar experimental conditions (with the addition of dimethyl sulfoxide (DMSO), 2% (v/v), required for dissolution of the compound), the reduction of aggregation is less evident when the peptide is treated with **1Pt**: it is about 35 and 20% at 1:1 and 1:5 peptide-to-metal compound molar ratios, respectively (Figure 2C). The differences between the behavior of the two Pt complexes are more evident when the ThT profiles of $A\beta_{25-35}$ are compared: when the peptide is incubated with $\mathbf{1Pt_{dep}}$, the reduction of the aggregated fraction (70%) is essentially independent of the equivalents of the complex that were used (Figure 2B); on the contrary, when the peptide is treated with **1Pt**, the behavior is similar to that observed in the experiments carried out with $A\beta_{21-40}$. The suppressive effect of $A\beta_{25-35}$ aggregation exerted by **1Pt** is less significant than that of $\mathbf{1Pt_{dep}}$: the level of aggregation inhibition is comparable to that exhibited by $\mathbf{1Pt_{dep}}$ only

https://doi.org/10.1021/acs.inorgchem.1c03540
Inorg. Chem. 2022, 61, 3540−3552

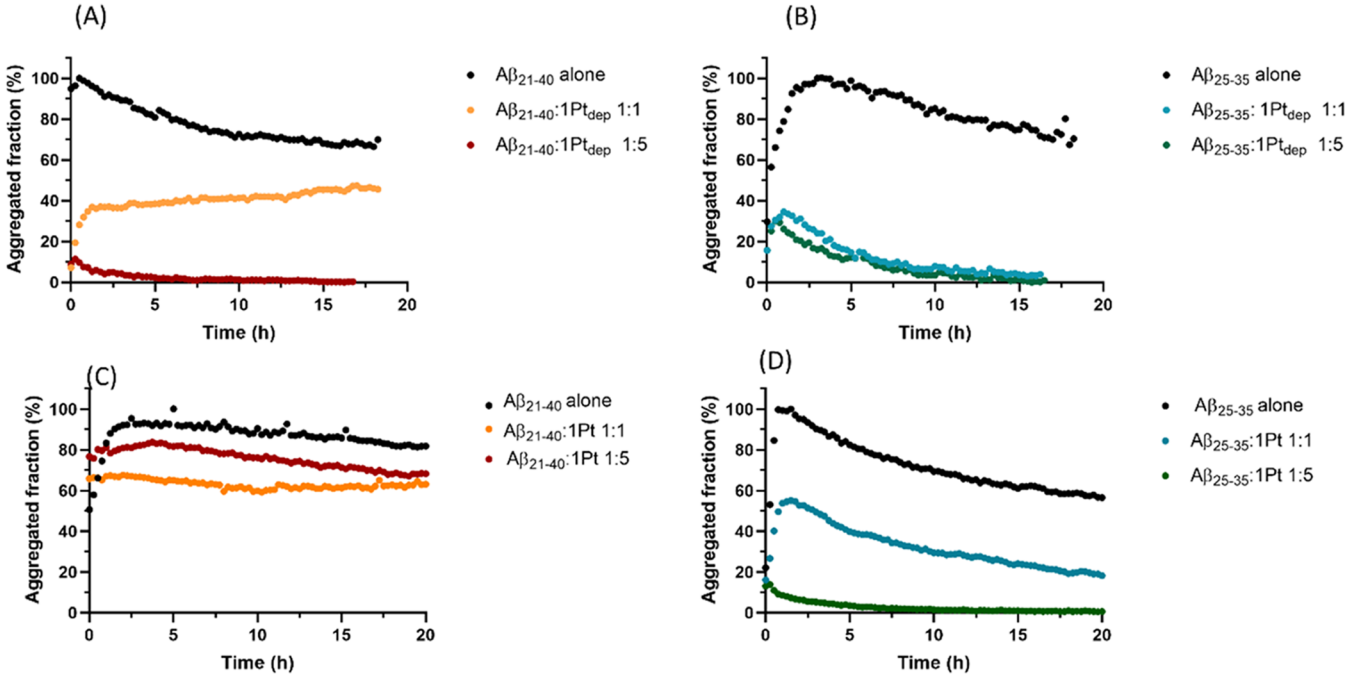

Figure 2. Time course of ThT fluorescence emission intensity of (A, C) Aβ_{21-40} and (B, D) Aβ_{25-35}, alone and upon incubation with (A, B) **1Pt$_{dep}$** or (C, D) **1Pt** at indicated peptide-to-metal molar ratios. Values are the average of two measurements.

when the peptide-to-metal compound molar ratio is 1:5 (Figure 2D). Noticeably, a preliminary experiment employing the entire Aβ_{1-42} sequence as aggregating polypeptide,[51] reported in Figure S1, confirmed the ability of **1Pt$_{dep}$** to inhibit amyloid aggregation, at a 1:5 Aβ_{1-42}/**1Pt$_{dep}$** molar ratio. Future experiments will detail the different involvements of N- and C-terminal regions in this inhibitory process.

Electrospray Ionization Mass Spectrometry (ESI-MS) Analysis of Adducts between Aβ_{21-40}, Aβ_{25-35}, and Pt(II) Complexes. Aβ_{21-40} and Aβ_{25-35} were incubated with Pt compounds (at 1:5 peptide-to-metal complex molar ratio) and the samples were analyzed by electrospray ionization mass spectrometry (ESI-MS); the peptides alone were analyzed as references. Signals of the b series for both peptides were generated from spontaneous in-source fragmentation events (Figure S2A,B). The spectra (Figures 3 and 4) of samples containing metal complexes were registered at two times of incubation, $t = 0$ (Figures 3A and 4A) and $t = 24$ h (Figures 3B and 4B). The species recorded in Aβ_{21-40} and Aβ_{25-35} spectra are summarized in Tables 2 and 3, respectively.

1Pt$_{dep}$ appears to be able to bind to both peptides by substituting the equatorial 2,9-dimethyl-1,10-phenanthroline (Dmphen) and ethylene ligands, as demonstrated by the presence of the peak at m/z 1190.06 (Table 2, C component MW = 2378.12 Da) for Aβ_{21-40} (Figure 3B) and the peak at m/z 777.37 (Table 3, B component MW = 1552.75 Da) for Aβ_{25-35} (Figure 4). Moreover, each peptide also showed the ability to form adducts where the metal complex lacks the glucosyl axial ligand, as revealed by the presence of the species showing molecular weights of 2134.02 Da (component B in Table 2) and 2411.73 Da (component C in Table 3) and corresponding to the adducts generated by Aβ_{21-40} and Aβ_{25-35}. In addition to these common features, several relevant differences emerge from the analysis of the spectra: the first difference is regarding the kinetics of adduct formation. Indeed, contrary to that found for Aβ_{21-40}, Aβ_{25-35} peptide spectra (Figure 4A) show the formation of adducts at the beginning of incubation ($t = 0$). Peaks due to these adducts were assigned to Aβ_{25-35} bound to the **1Pt$_{dep}$** fragment carrying solely the glucosyl (component A, m/z = 769.86) or both the axial ligands (component B, m/z = 777.37). Moreover, the amount of both adducts increases over time. Aβ_{21-40} showed the formation of the adduct containing glucosyl and methyl ligands only after 24 h (component C, m/z = 1190.06, Figure 3B, Table 2).

At the longest time, an additional distinguishing feature of Aβ_{25-35} samples was further detected: the occurrence of species with MWs 2411.73 ± 0.49 and 2655.49 ± 0.25 Da (components C and D, respectively, Table 3), which were both attributed to the formation of adducts with a 2:1 peptide/metal complex stoichiometry. Component D (2655.49 Da) was attributed to the adduct containing **1Pt$_{dep}$** lacking the equatorial ligands and carrying two Aβ_{25-35} chains bound in a monodentate mode, while component C, showing 2411.73 Da as MW, consisted of the same species lacking also the axial sugar moiety. The simultaneous binding of two Aβ_{25-35} sequences is not encountered in Aβ_{21-40} samples. Conversely, only Aβ_{21-40} exhibited an adduct with naked Pt(II) ions as indicated by the presence of component A (m/z = 1060.00, Figure 3B, Table 2).

The analysis of the b series in the spectra of the peptide with **1Pt$_{dep}$** provided insights into the peptide fragments mainly involved in the adduct formation. In the spectra of Aβ_{25-35} with **1Pt$_{dep}$** (Figure 4), the monocharged signals at m/z 925.31 and 941.35 were due to the b_5 element obtained by Aβ_{25-35} + (Pt + sugar) and Aβ_{25-35} + (Pt + sugar + Me) fragmentation, respectively.

The presence of the b series fragments suggested that the N-terminal stretch of the peptide is mainly responsible for the binding. Similarly, the b series signals were encountered also in the spectra of Aβ_{21-40} adducts. The doubly charged signals at m/z 1001.95, 1010.59, and 1133.03 (Figure 3B) are in

https://doi.org/10.1021/acs.inorgchem.1c03540
Inorg. Chem. 2022, 61, 3540−3552

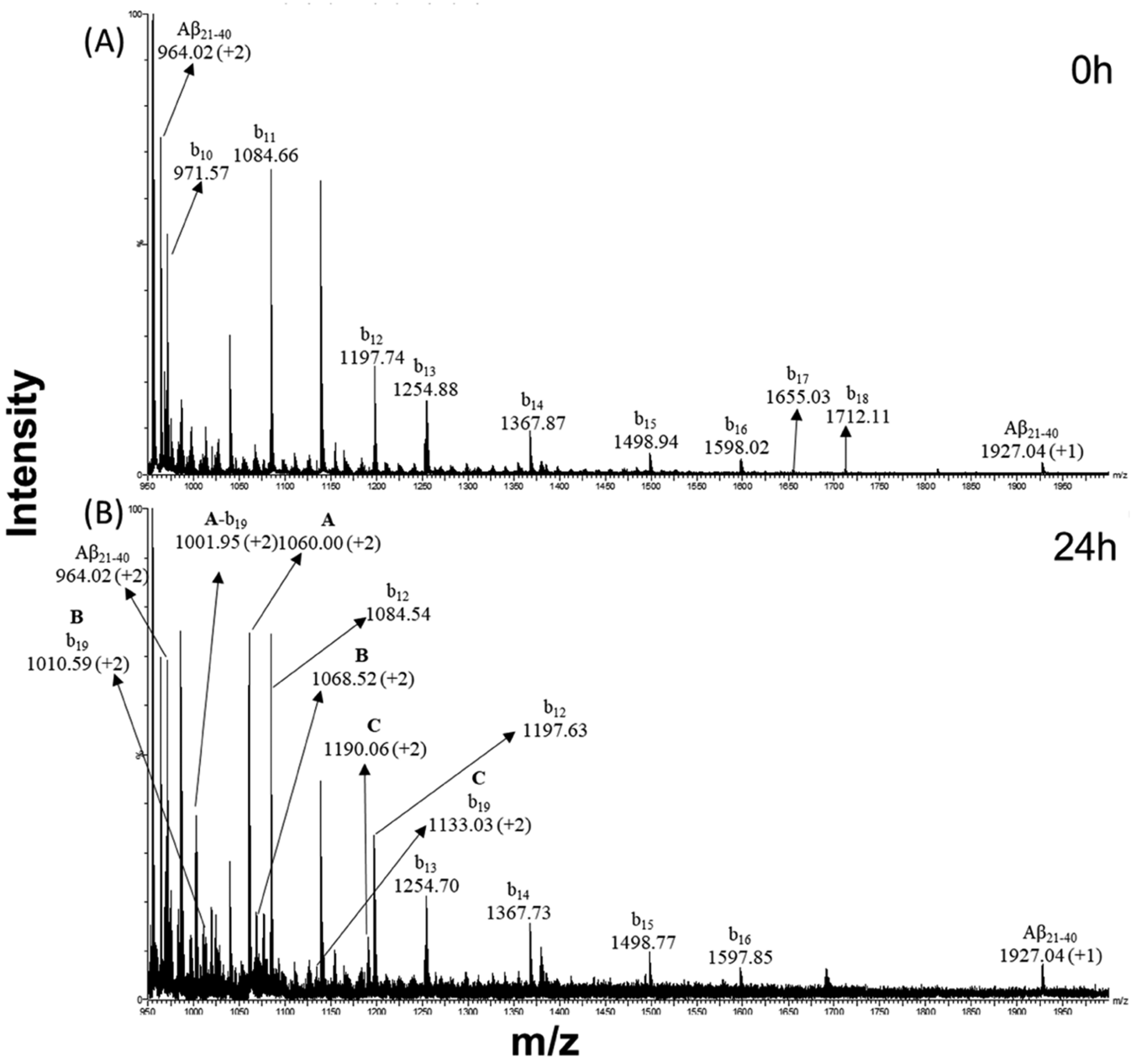

Figure 3. ESI-MS spectra of the Aβ_{21-40} peptide incubated with **1Pt$_{dep}$** for (A) 0 h and (B) 24 h. Signals from ion fragmentation are also reported.

accordance with the b_{19} signal of Aβ_{21-40} bound to naked Pt(II), Pt + Me, and Pt + sugar + Me fragments, as previously reported.[44]

ESI-MS analysis was also carried out by incubating β-peptides with the **1Pt** complex. In this case, no peaks deriving from adducts were detected over the time for Aβ_{21-40} (Figure S3). A peak was found only for Aβ_{25-35}, in the spectral background, consistent with a 2:1 stoichiometry and compatible with an adduct of the Pt(II) complex with both the axial ligands (Figure S4). These findings confirm the results already described by Annunziata et al.:[48] small variations in terms of the ligand structure, such as the presence of protecting groups, are able to substantially modify the binding capacity of a metal compound toward the same biomolecule. On the basis of these results, we further investigated only the ability of **1Pt$_{dep}$** to modulate the amyloid aggregation of Aβ peptides.

Spectroscopic Investigations of Adducts with 1Pt$_{dep}$. Ultraviolet−visible (UV−vis) absorption spectroscopy was employed to detect potential variations of the ligand field of **1Pt$_{dep}$** induced by the presence of amyloid peptides. In agreement with literature studies on Pt(II)−diimine complexes,[52,53] the spectra are characterized by the presence of the $\pi \rightarrow \pi^*$ intraligand and Pt(5d) $\rightarrow \pi^*$ metal-to-ligand charge transfer (MLCT) transitions in the 200−400 nm region. As reported in Figure 5 upper panel, an enhancement of absorbances upon increasing the amounts of both Aβ_{25-35} (Figure 5A) and Aβ_{21-40} (Figure 5B) is observable: this suggests that a mechanism of substitution of ligands around the Pt center occurred. This titration, in the case of Aβ_{25-35}, allowed us to estimate EC_{50} = 93.7 ± 0.2 μM, through the fitting of absorbance values at 330 nm (inset of Figure 5A). This value is comparable to that observed in other studies of metal complex/amyloid peptide systems.[41,44] Data fitting did

https://doi.org/10.1021/acs.inorgchem.1c03540
Inorg. Chem. 2022, 61, 3540−3552

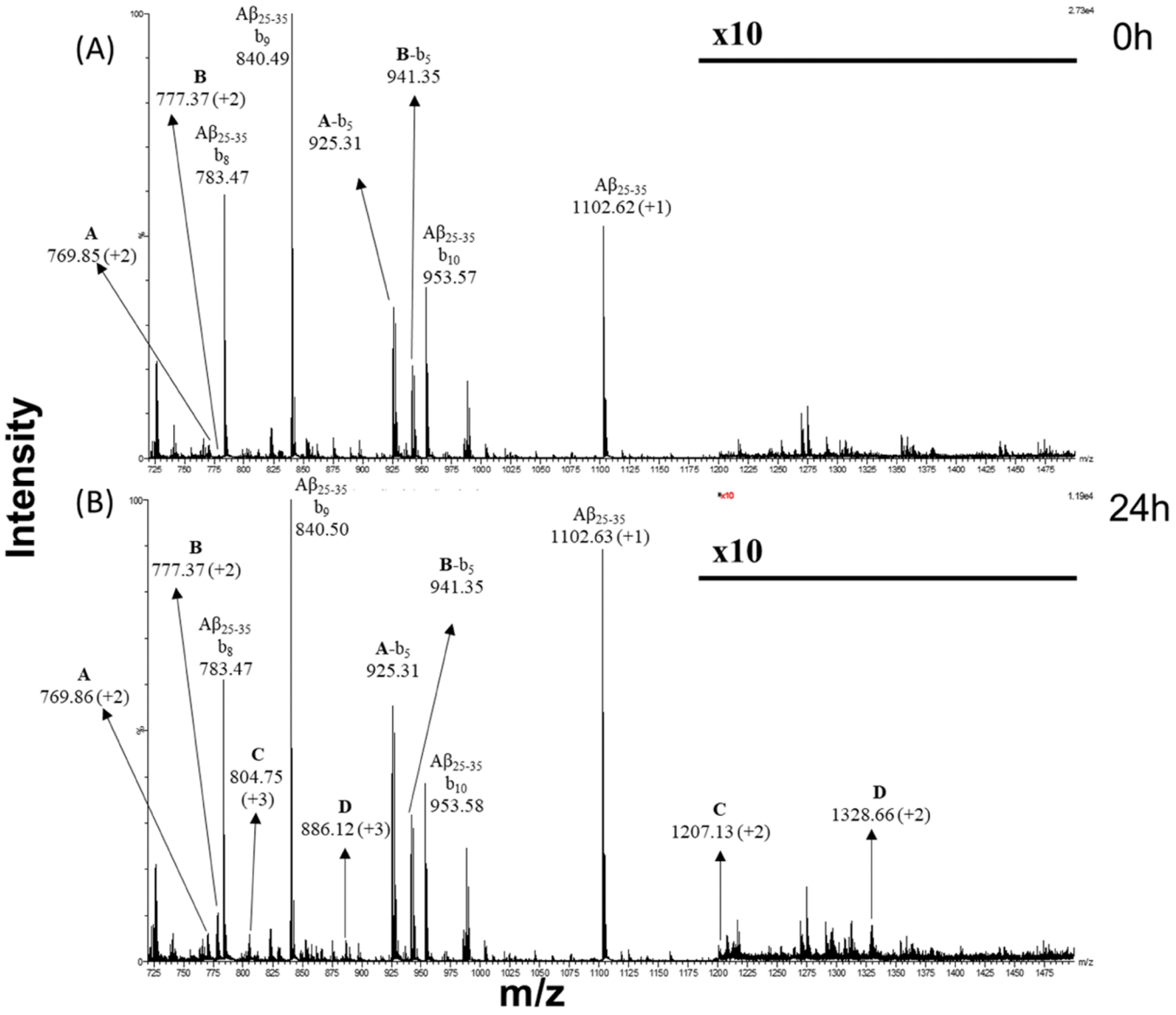

Figure 4. ESI-MS spectra of the Aβ_{25-35} peptide incubated with **1Pt$_{dep}$** for (A) 0 h and (B) 24 h. Signals from ion fragmentation are also reported. The m/z range between 1200 and 1500 is 10 times magnified.

Table 2. Results of ESI-MS of the Aβ_{21-40} Peptide Incubated for 0 and 24 h with 1Pt$_{dep}$[a]

component	experimental m/z, (charge state)	experimental monoisotopic mass (Da)	theoretical monoisotopic mass (Da)	Aβ_{21-40}-Pt adducts	time (h)
	964.02 (+2)	1926.03 ± 0.01	1926.01	Aβ_{21-40}	
	1927.04 (+1)				
A	1060.00 (+2)	2118.00	2121.09	Aβ_{21-40} + Pt(II)	24
B	1068.01 (+2)	2134.02	2136.12	Aβ_{21-40} + (Pt + Me)	24
C	1190.06 (+2)	2378.12	2379.36	Aβ_{21-40} + (Pt + sugar + Me)	24

[a]The m/z experimental values, experimental and theoretical monoisotopic molecular weights (MWs), and relative species are reported. In the "component" column, the labels of species in Figure 3 are reported. Me: methyl ligand; sugar: glucosyl ligand.

not converge in the case of Aβ_{21-40}, hampering the evaluation of the EC$_{50}$ value for this peptide (inset of Figure 5B).

To evaluate if the presence of **1Pt$_{dep}$** could have effects on the conformation of Aβ peptides, we registered CD spectra of freshly prepared samples and of the peptides incubated for 24 h with the metal compound. Spectra are reported in Figure 5. At t = 0, Aβ_{21-40} presented a substantial random coil profile, while Aβ_{25-35} presented a mixture of random coil and β-sheet signals;[54] after 24 h, for both sequences, a clear conformational transition toward β-structures occurred (Figure 5C,E), as often observed during amyloid aggregation.[44,55] Spectra registered in the presence of **1Pt$_{dep}$**, which exhibits a nonnull Cotton effect (Figure S5), at two different times, indicate the absence of the minimum at 220 nm typical of β-sheet structures (Figure 5D,F). This finding suggests that the presence of the Pt

https://doi.org/10.1021/acs.inorgchem.1c03540
Inorg. Chem. 2022, 61, 3540−3552

Table 3. Results of ESI-MS of the $A\beta_{25-35}$ Peptide Incubated for 0 and 24 h with $1Pt_{dep}$[a]

component	experimental m/z, (charge state)	experimental monoisotopic mass (Da)	theoretical monoisotopic mass (Da)	$A\beta_{25-35}$-Pt adducts	time (h)
	1102.63 (+1)	1101.63	1100.58	$A\beta_{25-35}$	
A	769.86 (+2)	1537.72	1538.91	$A\beta_{25-35}$ + (Pt + sugar)	0, 24
B	777.37 (+2)	1552.75	1553.94	$A\beta_{25-35}$ + (Pt + sugar + Me)	0, 24
C	804.75 (+3)	2411.73 ± 0.49	2411.28	2·($A\beta_{25-35}$) + (Pt + Me)	24
	1207.13 (+2)				
D	886.12 (+3),	2655.49 ± 0.25	2654.52	2·($A\beta_{25-35}$) + (Pt + sugar + Me)	24
	1328.66 (+2)				

[a]The m/z experimental values, experimental and theoretical monoisotopic molecular weights, and the relative species are reported. In the component column, the labels of species in Figure 4 are reported. Me: methyl ligand; sugar: glucosyl ligand.

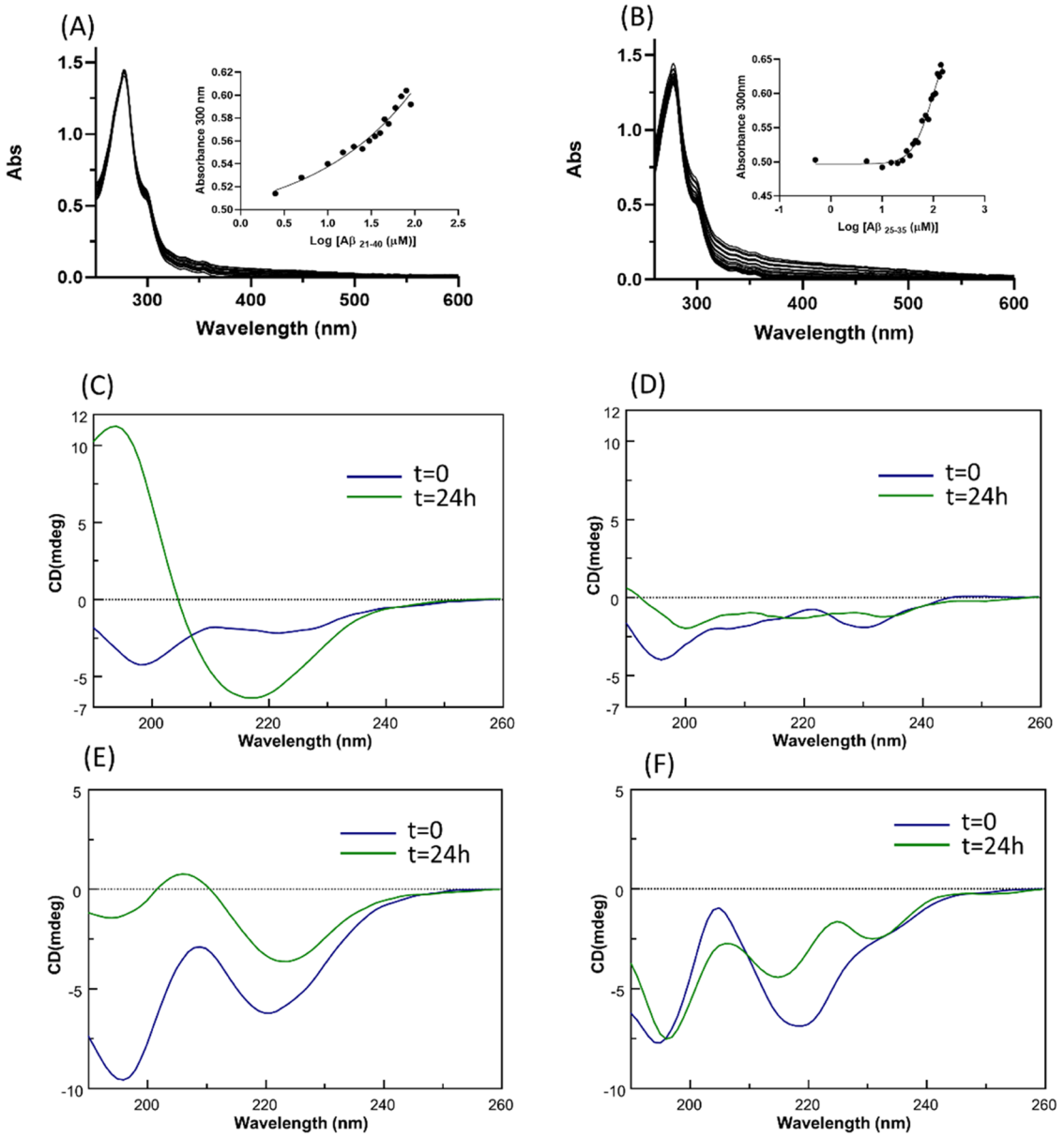

Figure 5. Spectroscopic investigations of the adducts of $A\beta_{21-40}$ and $A\beta_{25-35}$ with $\mathbf{1Pt_{dep}}$. Upper panel: absorption spectra of $\mathbf{1Pt_{dep}}$ upon the addition of increasing amounts of (A) $A\beta_{25-35}$ and (B) $A\beta_{21-40}$. As insets, UV intensities at indicated wavelengths *vs* log of $A\beta$ peptide concentrations. Lower panel: overlay of circular dichroism (CD) spectra of $A\beta_{21-40}$ (C) alone and (D) incubated with $\mathbf{1Pt_{dep}}$ at the 1:5 peptide/Pt(II) molar ratio and $A\beta_{25-35}$ (E) alone and (F) incubated with $\mathbf{1Pt_{dep}}$ at a 1:5 peptide/Pt(II) molar ratio.

complex causes the inhibition of the conformational transition that preludes fibrillization.

NMR Investigations. To gain further structural insights on the interaction between $\mathbf{1Pt_{dep}}$ and $A\beta$ peptides, NMR studies were carried out. We focused on $A\beta_{25-35}$ since its sequence is

https://doi.org/10.1021/acs.inorgchem.1c03540
Inorg. Chem. 2022, 61, 3540−3552

more influenced by the presence of the **1Pt$_{dep}$** complex than Aβ_{21-40}.

We first run one-dimensional (1D) [^{1}H] spectra, reported in Figure 6, of Aβ_{25-35} alone at t = 0 and 4 h from a freshly

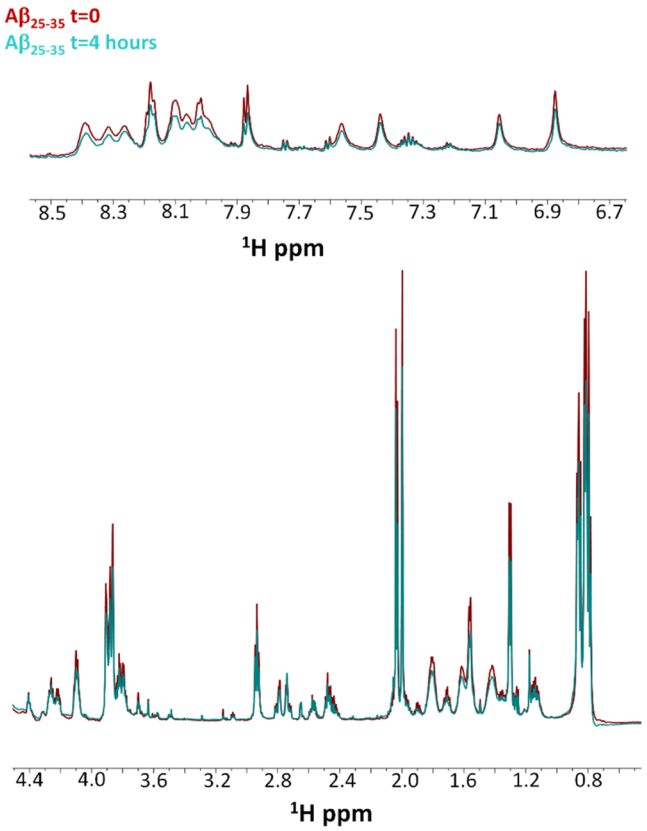

Figure 6. Comparison of 1D [^{1}H] spectra of Aβ_{25-35} alone at t = 0 (red) and 4 h (cyan). The H_N region is shown in the upper panel, the H_α and side chain proton region is reported in the lower panel.

prepared sample. Spectra at t = 0 and 4 h present rather sharp signals, except for the solvent-exposed H_N peaks (Figure 6 upper panel), indicating the presence of species with small molecular weights and a disordered organization. This is not surprising as large oligomers and protofibrils cannot be observed by solution NMR due to fast relaxation, while disaggregated and/or small oligomers are NMR visible.[56,57] After 4 h, a slight decrease of signal intensity is observed (Figure 6). This suggests that large aggregates are formed, although most of the peptide remains in the disaggregated and/or in small oligomer forms (Figure 6).

A two-dimensional (2D) [^{1}H, ^{1}H] total correlation spectroscopy (TOCSY) spectrum reported in Figure S6 allows us to distinguish side chain protons of different residues of Aβ_{25-35}. 1D [^{1}H] NMR spectra were also recorded for **1Pt$_{dep}$** alone at t = 0 and 4 h and are reported in Figure 7.

After 4 h, many changes occur in the spectrum: additional signals appear, and the peaks of the main compound decrease in intensity. New peaks are assigned to free ligands that are released from the metal coordination sphere. Indeed, previous ^{1}H NMR studies of the **1Pt** analogue compound conducted in DMSO-d_6 indicated that both Dmphen and ethylene could be displaced by solvent molecules leading, over time, to square-planar species.[48] In detail, the signal close to 0.0 ppm is due to Pt-CH_3 in a square-planar geometry, supporting the coex-

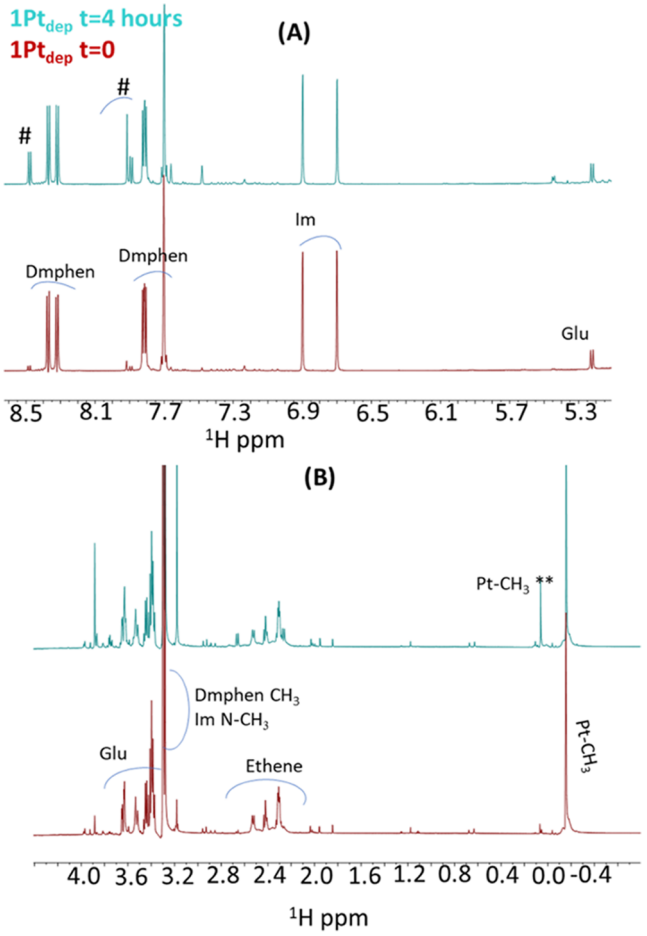

Figure 7. Comparison of 1D [^{1}H] spectra of **1Pt$_{dep}$** at t = 0 (red) and 4 h (cyan). Intervals of chemical shift: (A) 5.3−8.5 and (B) −0.4 to 4.0 ppm. Assignment of Pt ligands is reported at t = 0. Dmphen: 2,9-dimethyl-1,10-phenanthroline, Im: imidazole derivative, Glu: glucosyl unit. On the top cyan spectrum, peaks arising from free Dmphen are indicated by #, while ** refers to Pt-CH_3 in a square-planar complex.[48]

istence of square-planar along with the bipyramidal trigonal geometry that, however, is still predominant after 4 h[48] (Figure 7B).

1D [^{1}H] spectra were also acquired for Aβ_{25-35} in the presence of **1Pt$_{dep}$** (1:5 peptide/metal molar ratio). Spectra recorded at t = 0 and 4 h appear quite similar, indicating that no time effects are observable under NMR conditions (Figure S7). Interestingly, in the comparison of 1D [^{1}H] spectra of **1Pt$_{dep}$** at t = 0 and of **1Pt$_{dep}$** + Aβ_{25-35} at either t = 0 or 4 h, no relevant changes can be observed, clearly indicating a mutual influence between the complex and the peptide. Interestingly, it can be noted that the presence of Aβ_{25-35} stabilizes the bipyramidal trigonal geometry of the metal compound since ^{1}H signals from the **1Pt$_{dep}$** spectrum recorded at t = 0 can be overlayed with those present in the spectrum of **1Pt$_{dep}$** + Aβ_{25-35} at t = 4 h if one excludes minor chemical shift changes (Figure S8). By comparing 1D [^{1}H] spectra of Aβ_{25-35} alone and **1Pt$_{dep}$** + Aβ_{25-35} at t = 4 h, a few chemical shift changes could be noticed (Figure 8): these variations do not affect H_N (Figure 8A) and H_α (Figure 8B) protons but concern mainly with CH_2 (Figure 8C,D) and CH_3 (Figure 8E) side chain protons, except for the serine residue that seems unaffected (Figure 8B). The chemical shift changes indicate some

https://doi.org/10.1021/acs.inorgchem.1c03540
Inorg. Chem. 2022, 61, 3540−3552

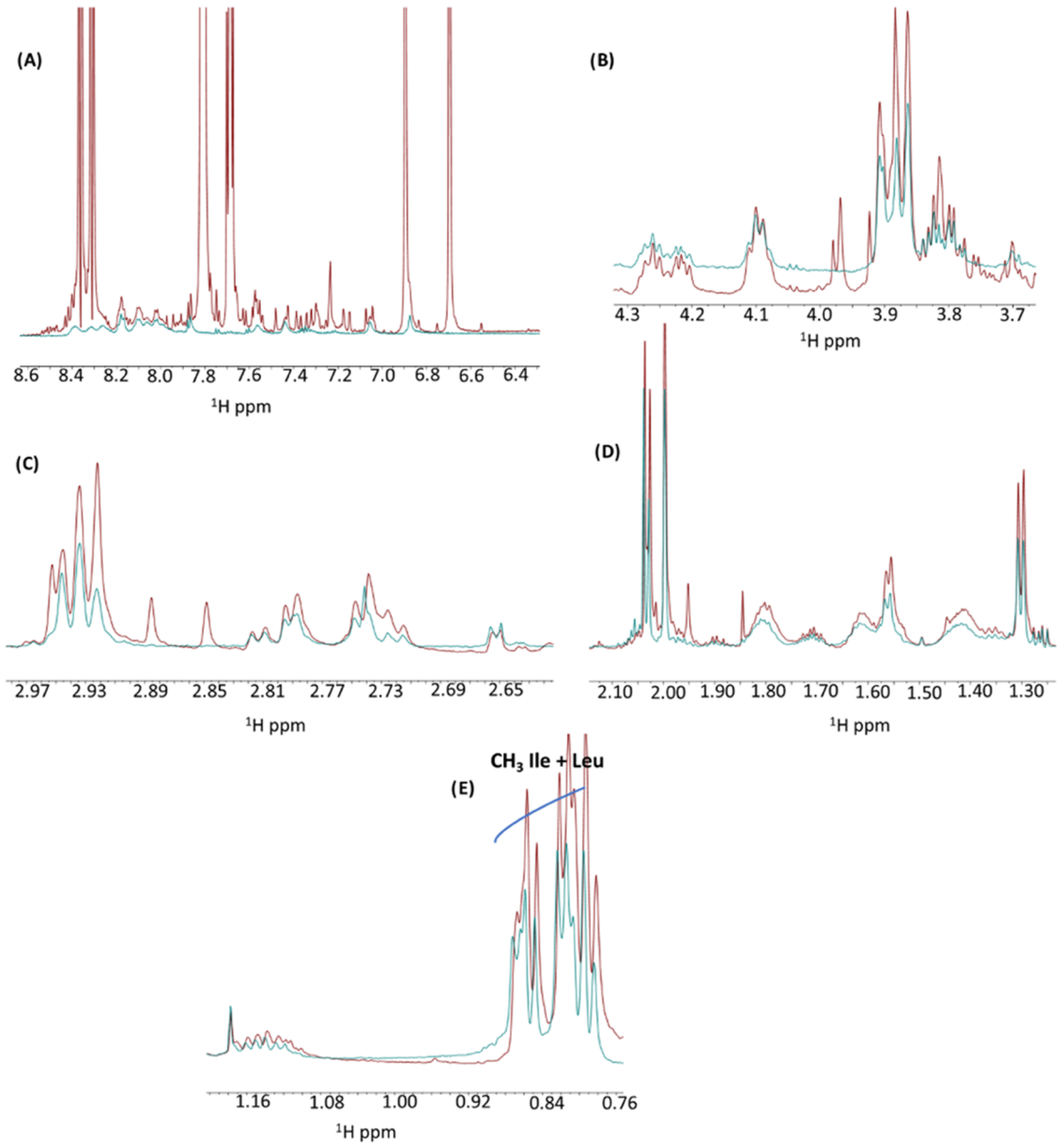

Figure 8. Overlay of 1D [^{1}H] spectra of $\mathbf{1Pt_{dep}}$ + Aβ_{25-35} (red) and Aβ_{25-35} alone (cyan) at t = 4 h. Different chemical shift regions are reported in each panel.

conformational variations induced in the Aβ_{25-35} peptide by the presence of $\mathbf{1Pt_{dep}}$.

Structural Analysis of Amyloid Fibers of Aβ-Derived Peptides in the Presence of $\mathbf{1Pt_{dep}}$. To get insights into the morphology of the aggregates derived from Aβ peptides in the presence and absence of $\mathbf{1Pt_{dep}}$, confocal and scanning electron microscopies (SEMs) were used. Confocal analysis of Aβ peptides alone presents typical amyloid fiber shapes (Figure 9A,G), while the presence of the metal complex at a 1:5 metal complex-to-peptide molar ratio determines the suppression of the fiber, favoring the formation of amorphous aggregates (Figure 9D,J). SEM experiments corroborate these results: micrographs registered at different magnifications (reported in Figure 9) delight the presence of well-structured fibers with an average diameter of 3.3 ± 1.0 × 10 μm and a length of 4.7 ± 0.8 × 10^2 μm for Aβ_{21-40} (Figure 9B,C) and a diameter of 24 ± 7 μm and a length of 8.1 ± 0.2 × 10^2 μm for Aβ_{25-35} (Figure 9H,I). The presence of $\mathbf{1Pt_{dep}}$ perturbs microstructure formation in this case as well: the microstructures appear immersed in the stub matrix, not a well defined and faintly visible event at high magnification values (Figure 9E,F,K,L).

EXPERIMENTAL SECTION

Reagent Syntheses. **1Pt** and $\mathbf{1Pt_{dep}}$[48] and Aβ_{21-40} and Aβ_{25-35} peptides[58] were synthesized as already reported, synthetic Aβ_{1-42} was purchased from Abcam, and related sequences are reported in Table 1. After purification, they were treated with 1,1,1,3,3,3-hexafluoro-2-propanol (HFIP) and then stored at −20 °C until use.

Fluorescence Assays. ThT fluorescence assays were performed at 25 °C, employing a peptide concentration of 100 μM for Aβ_{21-40} and 200 μM for Aβ_{25-35} in 10 mM phosphate buffer at pH 7.4, using a ThT final concentration of 50 μM, at different ratios with Pt(II) complexes (stock solutions 1 mM in water for $\mathbf{1Pt_{dep}}$ and in 100% DMSO for both complexes). ThT experiments that have been carried out with **1Pt** were acquired in solutions containing DMSO at 2% (v/v). In this solvent, **1Pt** is stable, as suggested by UV−vis absorption spectra collected as a function of time and reported in Figure S9. To

https://doi.org/10.1021/acs.inorgchem.1c03540
Inorg. Chem. 2022, 61, 3540−3552

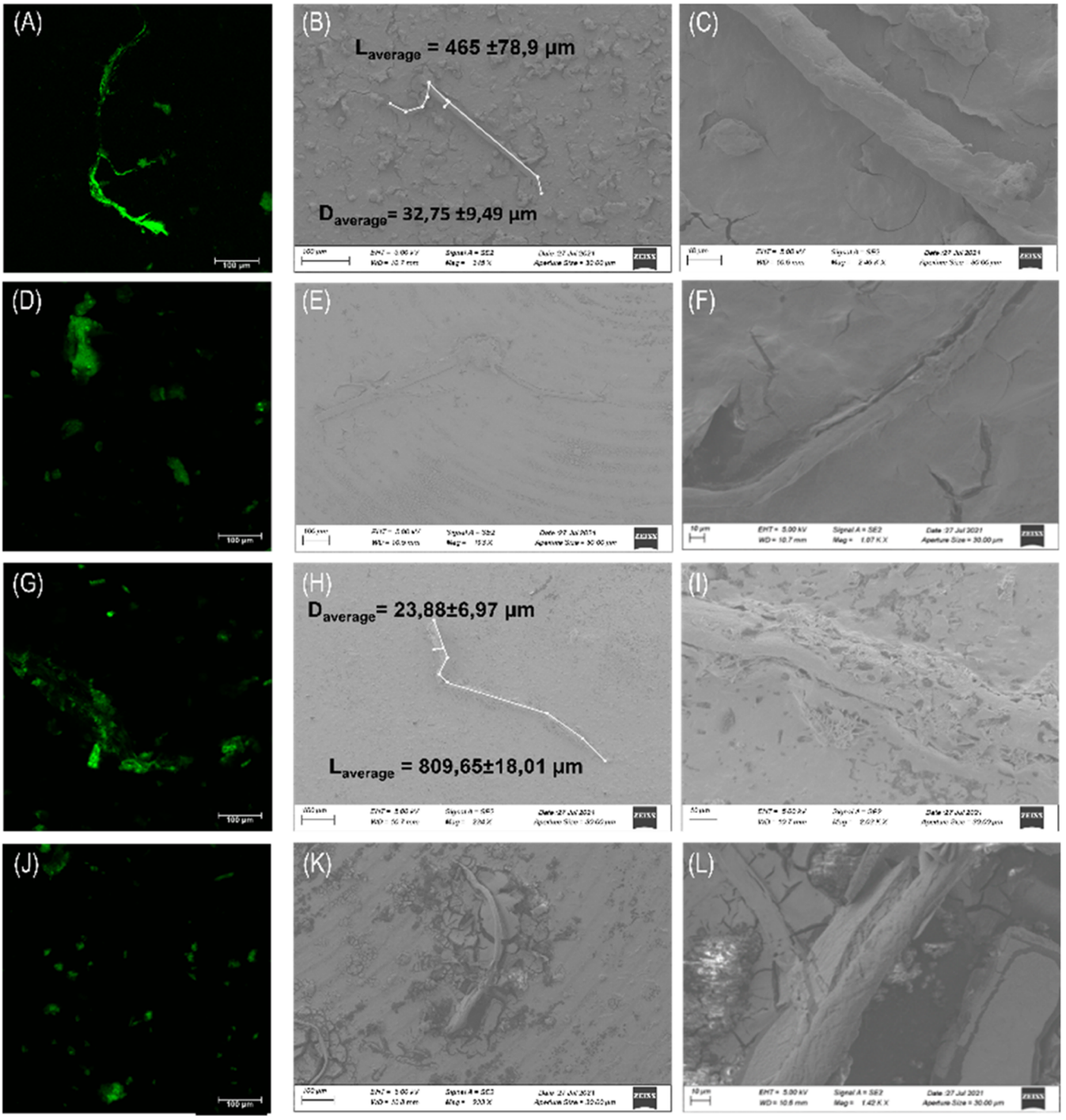

Figure 9. Microscopic studies of Aβ peptides in the absence and presence of $\mathbf{1Pt_{dep}}$. Confocal microscopy of ThT incubated systems: (A, G) Aβ_{21-40} and Aβ_{25-35} alone, (D) Aβ_{21-40}:$\mathbf{1Pt_{dep}}$, (J) Aβ_{25-35}:$\mathbf{1Pt_{dep}}$ both at a 1:5 ratio (λ_{exc} = 440 nm and λ_{emiss} between 460 and 600 nm). SEM micrographs of (B, C) Aβ_{21-40} and (E, F) Aβ_{21-40}:$\mathbf{1Pt_{dep}}$. (H, I) Aβ_{25-35} and (K, L) Aβ_{25-35}:$\mathbf{1Pt_{dep}}$ at 1:5, at (B, E, H, K) 100 μm and (C, F, I, L) 10 μm.

correctly compare the time course fluorescence intensities of the peptides in the presence of **1Pt** and $\mathbf{1Pt_{dep}}$, percentages of aggregated fractions are reported. Fluorescence was measured using a Jasco FP 8300 fluorescence spectrofluorometer in a 1 cm cuvette under magnetic stirring. The excitation wavelength was 440 nm and the emission wavelength was between 450 and 600 nm. A scanning speed of 100 nm/min was used. Spectra were recorded every 15 min at the indicated times and assays were performed in duplicates. The fluorescence intensity peak was determined at 482 nm.

Circular Dichroism. CD spectra of Aβ_{21-40} (50 μM) and Aβ_{25-35} (100 μM) in 10 mM phosphate buffer, alone or at a 1:2.5 peptide-to-metal complex molar ratio with $\mathbf{1Pt_{dep}}$, were registered on a Jasco J-815 spectropolarimeter (JASCO, Tokyo, Japan), in a 0.1 cm cuvette.

UV−Vis Absorption Spectroscopy. UV−vis spectra of $\mathbf{1Pt_{dep}}$ at increasing amounts of Aβ peptides were registered on a Nanodrop 2000c spectrophotometer (Thermo Scientific, Milan). The complex concentration was fixed at 50 μM. Peptides were added through the incorporation of 2.0 μL of peptide stock solution (500 μM) in water, kept at 0 °C. Spectra were recorded in the range of 260−600 nm after

https://doi.org/10.1021/acs.inorgchem.1c03540
Inorg. Chem. 2022, 61, 3540−3552

the peptide addition and 2 min under stirring. Upon addition, the metal complex-to-peptide molar ratio was 1:3 for both peptides. The estimation of the EC_{50} value was obtained from the nonlinear regression using the "dose−response stimulation equation" of GraphPad program and employing log [inhibitor] *vs* absorbance intensities as experimental data.[59]

ESI-MS Analysis. Solutions of Aβ_{21-40} and Aβ_{25-35} at a concentration of 50 μM in 15 mM ammonium acetate (pH = 6.8), at a 1:5 molar ratio with Pt(II) complexes, were incubated for two different time durations (0 and 24 h). The reaction mixtures were diluted 10 times with 15 mM ammonium acetate (pH = 6.8) and then analyzed using a Q-ToF Premier (Waters, Milliford, MA) mass spectrometer. For **1Pt$_{dep}$**, the *m*/*z* acquisition range spanned from 900 to 2500 *m*/*z* and from 500 to 1500 *m*/*z* for Aβ_{21-40} and Aβ_{25-35}. Differently, for **1Pt**, the Aβ_{25-35} *m*/*z* acquisition range was changed to 500−2000 *m*/*z*.

Scanning Electron Microscopy. SEM analysis was performed with an Ultra Plus FESEM scanning electron microscope (Zeiss, Germany). Samples (100 μL) containing Aβ_{21-40} (100 μM) and Aβ_{25-35} (200 μM), alone or mixed with **1Pt$_{dep}$** at a 1:5 ratio (10 mM phosphate buffer), were mounted on stub and gold-sputtered at 20 nm thickness using a HR208 Cressington sputter coater and analyzed at 10−15 kV with an SE2 detector, as already reported.[60,61] Fiber diameters and length were determined by ImageJ software.

Confocal Microscopy. Confocal microscopy analysis was performed by a Leica SP5 microscope using a HCX IRAPO L 40×/0.95 water objective, as previously reported.[62] Aβ_{21-40} (100 μM) and Aβ_{25-35} (200 μM) alone or with **1Pt$_{dep}$** at a 1:5 ratio incubated with ThT (50 μM) (50 mM phosphate buffer) were analyzed using an excitation of 440 nm and an emission between 460 and 600 nm.

NMR Assays. Analyzed NMR samples were (1) Aβ_{25-35} (400 μM), (2) **1Pt$_{dep}$** (2 mM), and (3) Aβ_{25-35}+ **1Pt$_{dep}$** (400 μM:2 mM nominal concentration) at t = 0 and 4 h of aggregation. Final volumes were of 540 μL (500 μL of sodium phosphate buffer pH 7.2 and 40 μL of D_2O (deuterium oxide, 98% D, Sigma-Aldrich, Milan, Italy). NMR spectra were recorded on a Bruker Avance 700 MHz spectrometer at 294 K. 1D [^{1}H] spectra were recorded with 64 scans. In addition, a 2D [^{1}H, ^{1}H] TOCSY[63] spectrum was recorded for Aβ_{25-35} with mixing time equal to 70 ms after 4 h. The 2D [^{1}H, ^{1}H] TOCSY spectrum was acquired with 58 scans, 128 free induction decays (FIDs) in t1, and 1024 data points in t2. Water suppression was achieved by presaturation. Spectra were processed and analyzed with TopSpin4.1.1 (Bruker, Italy). The 2D TOCSY spectrum was analyzed with NEASY[64] included in the Cara (computer-aided resonance assignment, http://www.nmr.ch/). Chemical shifts were referenced to the residual water peak at 4.75 ppm.

3-[4,5-Dimethylthiazol-2-yl]-2,5-diphenyl Tetrazolium Bromide (MTT) Assay. Human SH-SY5Y neuroblastoma cells were grown in Dulbecco's modified Eagle's medium (DMEM) (GIBCO, Paisley, U.K.) containing 10% heat-inactivated fetal bovine serum (FBS) (GIBCO), supplemented with 2 mM L-glutamine, 50 ng/mL streptomycin, and 50 units/mL penicillin and maintained in a humidified atmosphere (5% CO_2 at 37 °C). Once at 70−80% of confluence, cells were harvested with 0.25% trypsin (Sigma-Aldrich, St. Louis, MO). Aβ_{21-40} and Aβ_{25-35} alone or with **1Pt$_{dep}$** or **1Pt** at a 1:5 molar ratio, respectively, were incubated in 50 mM sodium phosphate buffer, pH 7.2, under stirring, and samples were taken at three different times: 0, 2, and 24 h. Peptides were added to the cells in culture media in 96-well plates at 100 μM and then incubated for 24 h at 37 °C. Cell viability was then assessed by the 3-(4,5-dimethylthiazol-2-yl)-2,5-diphenyl tetrazolium bromide (MTT) assay as previously described.[55,65]

CONCLUSIONS

The present study well reflects our recent focus on the applicability of metal-based anticancer drugs in the field of neurodegeneration: by assuming different amyloidogenic peptides as model systems of neurodegenerative proteins, we assessed the ability of several metal complexes with different metal ions (such as Pt, Ru, and Au) and diverse geometries (square-planar and octahedral) to act as inhibitors of self-aggregation processes.[40−42,44]

Herein, we have carried out several biophysical investigations to deepen, at the molecular level, the ability of two glycoconjugate Pt(II) bipyramidal complexes (Figure 1) to modulate amyloid aggregation. For its crucial involvement in AD, we have assumed as amyloid systems two fragments of the Aβ polypeptide: Aβ_{21-40} and Aβ_{25-35}.

In the first assay, ThT fluorescence of the peptides in the absence and presence of metal compounds over time has been registered. Data indicated a clear suppression of the aggregation process of both the peptides, mostly by water-soluble **1Pt$_{dep}$**, with a greater effect on the inhibition of aggregation of Aβ_{25-35}. ESI-MS and UV−vis absorption spectroscopy experiments outline that the inhibition of aggregation occurs through the formation of adducts between the Pt(II) bipyramidal complexes and Aβ peptides, through the insertion of peptides into the coordination sphere of the Pt center that implies the preferential release of the axial ligands, even if other exchanges can occur. ESI-MS analysis also indicated that in the case of the Aβ_{25-35}/**1Pt$_{dep}$** system, the metal complex can coordinate two peptide molecules at the same time, forming an adduct with 1:2 metal/peptide stoichiometry. This adduct cannot be formed in the case of Aβ_{21-40}, probably because of its longer sequence. Conversely, Aβ_{25-35} was the only sequence to provide an adduct, although of minimum intensity, with **1Pt**. This complex has a lower intrinsic ability to form adducts with the peptides, probably because of its minor capacity, when compared to its deprotected analogue, to form hydrogen bonds that could be important in the early stage of the peptide/metal complex recognition process that precedes the formation of the coordinative bond. Because of limited ability of **1Pt** to form adducts with the investigated peptides, we focused on **1Pt$_{dep}$** in further studies. From a conformational perspective, both CD and NMR experiments pointed out a deep mutual influence between the amyloidogenic peptide and **1Pt$_{dep}$**; indeed, the presence of the metal complex stabilizes monomeric forms/small aggregate forms of the peptide that do not evolve, during time, toward large aggregated species. In NMR assays, we observed that also the bipyramidal geometry of **1Pt$_{dep}$** is stabilized by the presence of Aβ_{25-35}. Finally, microscopy investigations confirmed all spectroscopic data showing that **1Pt$_{dep}$** suppresses the formation of amyloid fibers for both Aβ sequences. Unfortunately, the Pt complexes investigated in this study are not able to rescue the cytotoxicity induced by amyloid peptides, as reported in Figure S10. Thus, these compounds cannot be directly translated as neurodrugs, but, instead, they can be assumed as valid templates to develop more specific drugs, preferentially able to cross the brain barrier.

In conclusion, this study represents an important example of how biophysical characterization of the adducts formed upon the reaction of metallodrugs with amyloid peptides can highlight on their mechanism of aggregation inhibition and is promising for the application of analogous glycoconjugate Pt(II) bipyramidal derivatives as novel therapeutics in neurodegenerative diseases.

https://doi.org/10.1021/acs.inorgchem.1c03540
Inorg. Chem. 2022, 61, 3540−3552

■ ASSOCIATED CONTENT

Supporting Information

The Supporting Information is available free of charge at https://pubs.acs.org/doi/10.1021/acs.inorgchem.1c03540.

Time course of ThT fluorescence emission intensity of $A\beta_{1-42}$, alone and upon incubation with $\mathbf{1Pt}_{dep}$ at the indicated peptide-to-metal molar ratio: the values are the average of two measurements (Figure S1); ESI-MS spectra of $A\beta_{21-40}$ and $A\beta_{25-35}$ alone (Figure S2); ESI-MS spectra of the $A\beta_{21-40}$ peptide incubated with **1Pt** for 0 h and 24 h (Figure S3); ESI-MS spectra of the $A\beta_{25-35}$ peptide incubated with **1Pt** for 0 h and 24 h (Figure S4); overlay of CD spectra at 0 and 24 h of $\mathbf{1Pt}_{dep}$ (Figure S5); 2D [1H, 1H] TOCSY spectrum of $A\beta_{25-35}$ recorded at t = 4 h (Figure S6); overlay of 1D [1H] NMR spectra of $\mathbf{1Pt}_{dep}$ plus $A\beta_{25-35}$ (Figure S7); comparison between 1D [^{1}H] NMR spectra of $\mathbf{1Pt}_{dep}$ alone at t = 0 and $\mathbf{1Pt}_{dep}$ in the presence of $A\beta_{25-35}$ at t = 4 h (Figure S8); time course UV−vis spectra of **1Pt** at 50 μM in 2% DMSO phosphate buffer, 10 mM, at pH 7.4 (Figure S9); survival of SH-SY5Y cells treated with $A\beta_{21-40}$ and $A\beta_{25-35}$ (100 μM) alone or with $\mathbf{1Pt}_{dep}$ or **1Pt** at the 1:5 molar ratio at three time points: 0, 2, and 24 h; cells with peptides were incubated for 24 h and then processed for the MTT test ($^*p < 0.05$, $^{**}p < 0.005$, $^{\#}p < 0.001$, and $^{\&}p < 0.0001$ at statistical analysis of one experiment performed in triplicates) (Figure S10) (PDF)

■ AUTHOR INFORMATION

Corresponding Authors

Maria Monti − *Department of Chemical Sciences, University of Naples "Federico II", 80126 Naples, Italy; CEINGE Biotecnologie Avanzate S.c.a r.l., "University of Naples Federico II", 80131 Naples, Italy;* orcid.org/0000-0002-7775-7154; Phone: +39-081-674474; Email: montimar@unina.it

Daniela Marasco − *Department of Pharmacy, University of Naples "Federico II", 80131 Naples, Italy; Institute of Biostructures and Bioimaging - CNR, 80134 Naples, Italy;* orcid.org/0000-0002-6618-2949; Phone: +39-081-2532043; Email: daniela.marasco@unina.it

Authors

Sara La Manna − *Department of Pharmacy, University of Naples "Federico II", 80131 Naples, Italy*

Marilisa Leone − *Institute of Biostructures and Bioimaging - CNR, 80134 Naples, Italy;* orcid.org/0000-0002-3811-6960

Ilaria Iacobucci − *Department of Chemical Sciences, University of Naples "Federico II", 80126 Naples, Italy; CEINGE Biotecnologie Avanzate S.c.a r.l., "University of Naples Federico II", 80131 Naples, Italy*

Alfonso Annuziata − *Department of Chemical Sciences, University of Naples "Federico II", 80126 Naples, Italy*

Concetta Di Natale − *Interdisciplinary Research Centre on Biomaterials (CRIB), Department of Ingegneria Chimica del Materiali e della Produzione Industriale (DICMAPI), University "Federico II", 80125 Naples, Italy;* orcid.org/0000-0002-2874-6539

Elena Lagreca − *Interdisciplinary Research Centre on Biomaterials (CRIB), Department of Ingegneria Chimica del Materiali e della Produzione Industriale (DICMAPI), University "Federico II", 80125 Naples, Italy*

Anna Maria Malfitano − *Department of Translational Medical Science, University of Naples "Federico II", 80131 Naples, Italy*

Francesco Ruffo − *Department of Chemical Sciences, University of Naples "Federico II", 80126 Naples, Italy;* orcid.org/0000-0003-1624-079X

Antonello Merlino − *Department of Chemical Sciences, University of Naples "Federico II", 80126 Naples, Italy;* orcid.org/0000-0002-1045-7720

Complete contact information is available at: https://pubs.acs.org/10.1021/acs.inorgchem.1c03540

Author Contributions

S.L.M. synthesized peptides and performed fluorescence, UV, and CD studies, I.I. and M.M. performed ESI experiments. M.L. performed NMR studies, E.L. and C.D.N. conducted SEM assays, A.A. and F.R. synthesized and characterized the metal complexes. D.M., A.M., and M.M. designed the concept and supervised the experiments. M.M., A.M., and D.M. wrote the manuscript. All authors have read and approved the final version of the manuscript

Notes

The authors declare no competing financial interest.

■ ACKNOWLEDGMENTS

S.L.M. was supported by the AIRC fellowship for Italy.

■ REFERENCES

(1) Nie, Q.; Du, X.-g.; Geng, M.-y. Small molecule inhibitors of amyloid β peptide aggregation as a potential therapeutic strategy for Alzheimer's disease. *Acta Pharmacol. Sin.* **2011**, *32*, 545−551.

(2) Giuffrida, M. L.; Caraci, F.; Pignataro, B.; Cataldo, S.; De Bona, P.; Bruno, V.; Molinaro, G.; Pappalardo, G.; Messina, A.; Palmigiano, A.; et al. β-amyloid monomers are neuroprotective. *J. Neurosci.* **2009**, *29*, 10582−10587.

(3) Marasco, D.; Scognamiglio, P. L. Identification of inhibitors of biological interactions involving intrinsically disordered proteins. *Int. J. Mol. Sci.* **2015**, *16*, 7394−7412.

(4) Nguyen, P. H.; Ramamoorthy, A.; Sahoo, B. R.; Zheng, J.; Faller, P.; Straub, J. E.; Dominguez, L.; Shea, J. E.; Dokholyan, N. V.; De Simone, A.; Ma, B.; Nussinov, R.; Najafi, S.; Ngo, S. T.; Loquet, A.; Chiricotto, M.; Ganguly, P.; McCarty, J.; Li, M. S.; Hall, C.; Wang, Y.; Miller, Y.; Melchionna, S.; Habenstein, B.; Timr, S.; Chen, J.; Hnath, B.; Strodel, B.; Kayed, R.; Lesne, S.; Wei, G.; Sterpone, F.; Doig, A. J.; Derreumaux, P. Amyloid Oligomers: A Joint Experimental/Computational Perspective on Alzheimer's Disease, Parkinson's Disease, Type II Diabetes, and Amyotrophic Lateral Sclerosis. *Chem. Rev.* **2021**, *121*, 2545−2647.

(5) Reddy, P. H.; Beal, M. F. Amyloid beta, mitochondrial dysfunction and synaptic damage: implications for cognitive decline in aging and Alzheimer's disease. *Trends Mol. Med.* **2008**, *14*, 45−53.

(6) Ruan, L.; Kang, Z.; Pei, G.; Le, Y. Amyloid deposition and inflammation in APPswe/PS1dE9 mouse model of Alzheimer's disease. *Curr. Alzheimer Res.* **2009**, *6*, 531−540.

(7) Jokar, S.; Khazaei, S.; Behnammanesh, H.; Shamloo, A.; Erfani, M.; Beiki, D.; Bavi, O. Recent advances in the design and applications of amyloid-beta peptide aggregation inhibitors for Alzheimer's disease therapy. *Biophys. Rev.* **2019**, *11*, 901−925.

(8) Estrada, L.; Soto, C. Disrupting β-amyloid aggregation for Alzheimer disease treatment. *Curr. Top. Med. Chem.* **2007**, *7*, 115−126.

(9) Pagano, K.; Tomaselli, S.; Molinari, H.; Ragona, L. Natural Compounds as Inhibitors of Aβ Peptide Aggregation: Chemical

Requirements and Molecular Mechanisms. *Front. Neurosci.* **2020**, *14*, No. 619667.
(10) Ghosh, N.; Kundu, L. M. Breaker peptides against amyloid-β aggregation: a potential therapeutic strategy for Alzheimer's disease. *Future Med. Chem.* **2021**, *13*, 1767−1794.
(11) Salahuddin, P.; Khan, R. H.; Furkan, M.; Uversky, V. N.; Islam, Z.; Fatima, M. T. Mechanisms of amyloid proteins aggregation and their inhibition by antibodies, small molecule inhibitors, nanoparticles, and nano-bodies. *Int. J. Biol. Macromol.* **2021**, *186*, 580−590.
(12) Marasco, D.; Vicidomini, C.; Krupa, P.; Cioffi, F.; Huy, P. D. Q.; Li, M. S.; Florio, D.; Broersen, K.; De Pandis, M. F.; Roviello, G. N. Plant isoquinoline alkaloids as potential neurodrugs: A comparative study of the effects of benzo[c]phenanthridine and berberine-based compounds on beta-amyloid aggregation. *Chem.-Biol. Interact.* **2021**, *334*, No. 109300.
(13) Andrade, S.; Ramalho, M. J.; Loureiro, J. A.; Pereira, M. dC. Natural compounds for Alzheimer's disease therapy: a systematic review of preclinical and clinical studies. *Int. J. Mol. Sci.* **2019**, *20*, No. 2313.
(14) Scognamiglio, P. L.; Di Natale, C.; Perretta, G.; Marasco, D. From peptides to small molecules: an intriguing but intricated way to new drugs. *Curr. Med. Chem.* **2013**, *20*, 3803−3817.
(15) Russo, A.; Aiello, C.; Grieco, P.; Marasco, D. Targeting "Undruggable" Proteins: Design of Synthetic Cyclopeptides. *Curr. Med. Chem.* **2016**, *23*, 748−762.
(16) Bartus, É.; Olajos, G.; Schuster, I.; Bozso, Z.; Deli, M. A.; Veszelka, S.; Walter, F. R.; Datki, Z.; Szakonyi, Z.; Martinek, T. A.; Fulop, L. Structural Optimization of Foldamer-Dendrimer Conjugates as Multivalent Agents against the Toxic Effects of Amyloid Beta Oligomers. *Molecules* **2018**, *23*, No. 2523.
(17) McLaurin, J.; Cecal, R.; Kierstead, M. E.; Tian, X.; Phinney, A. L.; Manea, M.; French, J.; Lambermon, M. H.; Darabie, A. A.; Brown, M. E.; et al. Therapeutically effective antibodies against amyloid-β peptide target amyloid-β residues 4−10 and inhibit cytotoxicity and fibrillogenesis. *Nat. Med.* **2002**, *8*, 1263−1269.
(18) Permanne, B.; Adessi, C.; Saborio, G. P.; Fraga, S.; Frossard, M. J.; Van Dorpe, J.; Dewachter, I.; Banks, W. A.; Van Leuven, F.; Soto, C. Reduction of amyloid load and cerebral damage in transgenic mouse model of Alzheimer's disease by treatment with a β-sheet breaker peptide. *FASEB J.* **2002**, *16*, 860−862.
(19) Fawzi, N. L.; Phillips, A. H.; Ruscio, J. Z.; Doucleff, M.; Wemmer, D. E.; Head-Gordon, T. Structure and dynamics of the Aβ21−30 peptide from the interplay of NMR experiments and molecular simulations. *J. Am. Chem. Soc.* **2008**, *130*, 6145−6158.
(20) Lazo, N. D.; Grant, M. A.; Condron, M. C.; Rigby, A. C.; Teplow, D. B. On the nucleation of amyloid β-protein monomer folding. *Protein Sci.* **2005**, *14*, 1581−1596.
(21) Huang, S.-H.; Ke, S.-C.; Lin, T.-H.; Huang, H.-B.; Chen, Y.-C. Effect of C-terminal residues of Aβ on copper binding affinity, structural conversion and aggregation. *PLoS One* **2014**, *9*, No. e90385.
(22) McLaurin, J.; Kierstead, M. E.; Brown, M. E.; Hawkes, C. A.; Lambermon, M. H.; Phinney, A. L.; Darabie, A. A.; Cousins, J. E.; French, J. E.; Lan, M. F.; et al. Cyclohexanehexol inhibitors of Aβ aggregation prevent and reverse Alzheimer phenotype in a mouse model. *Nat. Med.* **2006**, *12*, 801−808.
(23) Son, G.; Lee, B. I.; Chung, Y. J.; Park, C. B. Light-triggered dissociation of self-assembled beta-amyloid aggregates into small, nontoxic fragments by ruthenium (II) complex. *Acta Biomater.* **2018**, *67*, 147−155.
(24) Suh, J. M.; Kim, G.; Kang, J.; Lim, M. H. Strategies Employing Transition Metal Complexes To Modulate Amyloid-beta Aggregation. *Inorg. Chem.* **2019**, *58*, 8−17.
(25) Wan, P. K.; Tong, K. C.; Lok, C. N.; Zhang, C.; Chang, X. Y.; Sze, K. H.; Wong, A. S. T.; Che, C. M. Platinum(II) N-heterocyclic carbene complexes arrest metastatic tumor growth. *Proc. Natl. Acad. Sci. U.S.A.* **2021**, *118*, No. e2025806118.
(26) Mjos, K. D.; Orvig, C. Metallodrugs in medicinal inorganic chemistry. *Chem. Rev.* **2014**, *114*, 4540−4563.
(27) Derrick, J. S.; Lee, J.; Lee, S. J.; Kim, Y.; Nam, E.; Tak, H.; Kang, J.; Lee, M.; Kim, S. H.; Park, K.; Cho, J.; Lim, M. H. Mechanistic Insights into Tunable Metal-Mediated Hydrolysis of Amyloid-beta Peptides. *J. Am. Chem. Soc.* **2017**, *139*, 2234−2244.
(28) Storr, T.; Gomes, L. M.; Bataglioli, J. C.; Jussila, A. J.; Smith, J. R.; Walsby, C. J. Modification of AB Peptide Aggregation via Covalent Binding of a Series of Ru (III) Complexes. *Front. Chem.* **2019**, *7*, No. 838.
(29) Barnham, K. J.; Kenche, V. B.; Ciccotosto, G. D.; Smith, D. P.; Tew, D. J.; Liu, X.; Perez, K.; Cranston, G. A.; Johanssen, T. J.; Volitakis, I.; Bush, A. I.; Masters, C. L.; White, A. R.; Smith, J. P.; Cherny, R. A.; Cappai, R. Platinum-based inhibitors of amyloid-beta as therapeutic agents for Alzheimer's disease. *Proc. Natl. Acad. Sci. U.S.A.* **2008**, *105*, 6813−6818.
(30) Sasaki, I.; Bijani, C.; Ladeira, S.; Bourdon, V.; Faller, P.; Hureau, C. Interference of a new cyclometallated Pt compound with Cu binding to amyloid-beta peptide. *Dalton Trans.* **2012**, *41*, 6404−6407.
(31) Collin, F.; Sasaki, I.; Eury, H.; Faller, P.; Hureau, C. Pt (II) compounds interplay with Cu (II) and Zn (II) coordination to the amyloid-β peptide has metal specific consequences on deleterious processes associated to Alzheimer's disease. *Chem. Commun.* **2013**, *49*, 2130−2132.
(32) Wang, X.; Cui, M.; Zhao, C.; He, L.; Zhu, D.; Wang, B.; Du, W. Regulation of aggregation behavior and neurotoxicity of prion neuropeptides by platinum complexes. *Inorg. Chem.* **2014**, *53*, 5044−5054.
(33) Wang, Y.; Feng, L.; Zhang, B.; Wang, X.; Huang, C.; Li, Y.; Du, W. Palladium complexes affect the aggregation of human prion protein PrP106-126. *Inorg. Chem.* **2011**, *50*, 4340−4348.
(34) Zhao, J.; Li, K.; Wan, K.; Sun, T.; Zheng, N.; Zhu, F.; Ma, J.; Jiao, J.; Li, T.; Ni, J.; Shi, X.; Wang, H.; Peng, Q.; Ai, J.; Xu, W.; Liu, S. Organoplatinum-Substituted Polyoxometalate Inhibits beta-amyloid Aggregation for Alzheimer's Therapy. *Angew. Chem., Int. Ed.* **2019**, *58*, 18032−18039.
(35) Xu, J.; Gong, G.; Huang, X.; Du, W. Schiff base oxovanadium complexes resist the assembly behavior of human islet amyloid polypeptide. *J. Inorg. Biochem.* **2018**, *186*, 60−69.
(36) Chan, T. G.; Ruehl, C. L.; Morse, S. V.; Simon, M.; Rakers, V.; Watts, H.; Aprile, F. A.; Choi, J. J.; Vilar, R. Modulation of amyloid-beta aggregation by metal complexes with a dual binding mode and their delivery across the blood-brain barrier using focused ultrasound. *Chem. Sci.* **2021**, *12*, 9485−9493.
(37) Gong, G.; Xu, J.; Huang, X.; Du, W. Influence of methionine-ruthenium complex on the fibril formation of human islet amyloid polypeptide. *J. Biol. Inorg. Chem.* **2019**, *24*, 179−189.
(38) Gong, G.; Du, W.; Xu, J.; Huang, X.; Yin, G. Regulation of heteronuclear Pt-Ru complexes on the fibril formation and cytotoxicity of human islet amyloid polypeptide. *J. Inorg. Biochem.* **2018**, *189*, 7−16.
(39) Józsa, É.; Osz, K.; Kallay, C.; de Bona, P.; Damante, C. A.; Pappalardo, G.; Rizzarelli, E.; Sovago, I. Nickel(II) and mixed metal complexes of amyloid-beta N-terminus. *Dalton Trans.* **2010**, *39*, 7046−7053.
(40) Florio, D.; Iacobucci, I.; Ferraro, G.; Mansour, A. M.; Morelli, G.; Monti, M.; Merlino, A.; Marasco, D. Role of the Metal Center in the Modulation of the Aggregation Process of Amyloid Model Systems by Square Planar Complexes Bearing 2-(2'-pyridyl)-benzimidazole Ligands. *Pharmaceuticals* **2019**, *12*, No. 154.
(41) Florio, D.; Malfitano, A. M.; Di Somma, S.; Mugge, C.; Weigand, W.; Ferraro, G.; Iacobucci, I.; Monti, M.; Morelli, G.; Merlino, A.; Marasco, D. Platinum(II) O,S Complexes Inhibit the Aggregation of Amyloid Model Systems. *Int. J. Mol. Sci.* **2019**, *20*, No. 829.
(42) Florio, D.; Cuomo, M.; Iacobucci, I.; Ferraro, G.; Mansour, A. M.; Monti, M.; Merlino, A.; Marasco, D. Modulation of Amyloidogenic Peptide Aggregation by Photoactivatable CO-Releasing Ruthenium(II) Complexes. *Pharmaceuticals* **2020**, *13*, No. 171.

https://doi.org/10.1021/acs.inorgchem.1c03540
Inorg. Chem. 2022, 61, 3540−3552

(43) Naldi, M.; Fiori, J.; Pistolozzi, M.; Drake, A. F.; Bertucci, C.; Wu, R.; Mlynarczyk, K.; Filipek, S.; De Simone, A.; Andrisano, V. , Amyloid beta-peptide 25-35 self-assembly and its inhibition: a model undecapeptide system to gain atomistic and secondary structure details of the Alzheimer's disease process and treatment. *ACS Chem. Neurosci.* **2012**, *3*, 952−962.
(44) La Manna, S.; Florio, D.; Iacobucci, I.; Napolitano, F.; Benedictis, I.; Malfitano, A. M.; Monti, M.; Ravera, M.; Gabano, E.; Marasco, D. A Comparative Study of the Effects of Platinum (II) Complexes on beta-Amyloid Aggregation: Potential Neurodrug Applications. *Int. J. Mol. Sci.* **2021**, *22*, No. 3015.
(45) Annunziata, A.; Cucciolito, M. E.; Esposito, R.; Ferraro, G.; Monti, D. M.; Merlino, A.; Ruffo, F. Five-Coordinate Platinum (II) Compounds as Potential Anticancer Agents. *Eur. J. Inorg. Chem.* **2020**, *2020*, 918−929.
(46) Pettenuzzo, A.; Pigot, R.; Ronconi, L. Metal-based glycoconjugates and their potential in targeted anticancer chemotherapy. *Metallodrugs* **2016**, *1*, 36−61.
(47) Annunziata, A.; Liberti, D.; Bedini, E.; Cucciolito, M. E.; Loreto, D.; Monti, D. M.; Merlino, A.; Ruffo, F. Square-Planar vs. Trigonal Bipyramidal Geometry in Pt(II) Complexes Containing Triazole-Based Glucose Ligands as Potential Anticancer Agents. *Int. J. Mol. Sci.* **2021**, *22*, No. 8704.
(48) Annunziata, A.; Cucciolito, M. E.; Esposito, R.; Imbimbo, P.; Petruk, G.; Ferraro, G.; Pinto, V.; Tuzi, A.; Monti, D. M.; Merlino, A.; et al. A highly efficient and selective antitumor agent based on a glucoconjugated carbene platinum (ii) complex. *Dalton Trans.* **2019**, *48*, 7794−7800.
(49) Biancalana, M.; Koide, S. Molecular mechanism of Thioflavin-T binding to amyloid fibrils. *Biochim. Biophys. Acta* **2010**, *1804*, 1405−1412.
(50) Xue, C.; Lin, T. Y.; Chang, D.; Guo, Z. Thioflavin T as an amyloid dye: fibril quantification, optimal concentration and effect on aggregation. *R. Soc. Open Sci.* **2017**, *4*, No. 160696.
(51) Zhang, T.; Loschwitz, J.; Strodel, B.; Nagel-Steger, L.; Willbold, D. Interference with Amyloid-beta Nucleation by Transient Ligand Interaction. *Molecules* **2019**, *24*, No. 2129.
(52) Dungey, K. E.; Thompson, B. D.; Kane-Maguire, N. A.; Wright, L. L. Photobehavior of (α-Diimine) dimesitylplatinum (II) Complexes. *Inorg. Chem.* **2000**, *39*, 5192−5196.
(53) Esposito, R.; Calvanese, L.; Cucciolito, M. E.; D'Auria, G.; Falcigno, L.; Fiorini, V.; Pezzella, P.; Roviello, G.; Stagni, S.; Talarico, G.; Ruffo, F. Oxidative Coupling of Imino, Amide Platinum (II) Complexes Yields Highly Conjugated Blue Dimers. *Organometallics* **2017**, *36*, 384−390.
(54) D'Ursi, A. M.; Armenante, M. R.; Guerrini, R.; Salvadori, S.; Sorrentino, G.; Picone, D. Solution structure of amyloid beta-peptide (25-35) in different media. *J. Med. Chem.* **2004**, *47*, 4231−4238.
(55) Di Natale, C.; Scognamiglio, P. L.; Cascella, R.; Cecchi, C.; Russo, A.; Leone, M.; Penco, A.; Relini, A.; Federici, L.; Di Matteo, A.; Chiti, F.; Vitagliano, L.; Marasco, D. Nucleophosmin contains amyloidogenic regions that are able to form toxic aggregates under physiological conditions. *FASEB J.* **2015**, *29*, 3689−3701.
(56) Pagano, K.; Tomaselli, S.; Molinari, H.; Ragona, L. Natural Compounds as Inhibitors of Abeta Peptide Aggregation: Chemical Requirements and Molecular Mechanisms. *Front. Neurosci.* **2020**, *14*, No. 619667.
(57) Sinopoli, A.; Giuffrida, A.; Tomasello, M. F.; Giuffrida, M. L.; Leone, M.; Attanasio, F.; Caraci, F.; De Bona, P.; Naletova, I.; Saviano, M.; Copani, A.; Pappalardo, G.; Rizzarelli, E. Ac-LPFFD-Th: A Trehalose-Conjugated Peptidomimetic as a Strong Suppressor of Amyloid-beta Oligomer Formation and Cytotoxicity. *ChemBioChem* **2016**, *17*, 1541−1549.
(58) Giuffrida, M. L.; Grasso, G.; Ruvo, M.; Pedone, C.; Saporito, A.; Marasco, D.; Pignataro, B.; Cascio, C.; Copani, A.; Rizzarelli, E. Abeta(25-35) and its C- and/or N-blocked derivatives: copper driven structural features and neurotoxicity. *J. Neurosci. Res.* **2007**, *85*, 623−633.
(59) Doti, N.; Scognamiglio, P. L.; Madonna, S.; Scarponi, C.; Ruvo, M.; Perretta, G.; Albanesi, C.; Marasco, D. New mimetic peptides of the kinase-inhibitory region (KIR) of SOCS1 through focused peptide libraries. *Biochem. J.* **2012**, *443*, 231−240.
(60) Florio, D.; Di Natale, C.; Scognamiglio, P. L.; Leone, M.; La Manna, S.; Di Somma, S.; Netti, P. A.; Malfitano, A. M.; Marasco, D. Self-assembly of bio-inspired heterochiral peptides. *Bioorg. Chem.* **2021**, *114*, No. 105047.
(61) Di Natale, C.; Natale, C. F.; Florio, D.; Netti, P. A.; Morelli, G.; Ventre, M.; Marasco, D. Effects of surface nanopatterning on internalization and amyloid aggregation of the fragment 264-277 of Nucleophosmin 1. *Colloids Surf., B* **2021**, *197*, No. 111439.
(62) Di Natale, C.; La Manna, S.; Avitabile, C.; Florio, D.; Morelli, G.; Netti, P. A.; Marasco, D. Engineered beta-hairpin scaffolds from human prion protein regions: Structural and functional investigations of aggregates. *Bioorg. Chem.* **2020**, *96*, No. 103594.
(63) Griesinger, C.; Otting, G.; Wuthrich, K.; Ernst, R. R. Clean TOCSY for proton spin system identification in macromolecules. *J. Am. Chem. Soc.* **1988**, *110*, 7870−7872.
(64) Bartels, C.; Xia, T.; Billeter, M.; Güntert, P.; Wüthrich, K. The program XEASY for computer-supported NMR spectral analysis of biological macromolecules. *J. Biomol. NMR* **1995**, *6*, 1−10.
(65) Di Natale, C.; La Manna, S.; Malfitano, A. M.; Di Somma, S.; Florio, D.; Scognamiglio, P. L.; Novellino, E.; Netti, P. A.; Marasco, D. Structural insights into amyloid structures of the C-terminal region of nucleophosmin 1 in type A mutation of acute myeloid leukemia. *Biochim. Biophys. Acta, Proteins Proteomics* **2019**, *1867*, 637−644.

https://doi.org/10.1021/acs.inorgchem.1c03540
Inorg. Chem. 2022, 61, 3540−3552